iScience

CellPress
OPEN ACCESS

Article

Aberrant sialylation in a patient with a *HNF1α* variant and liver adenomatosis

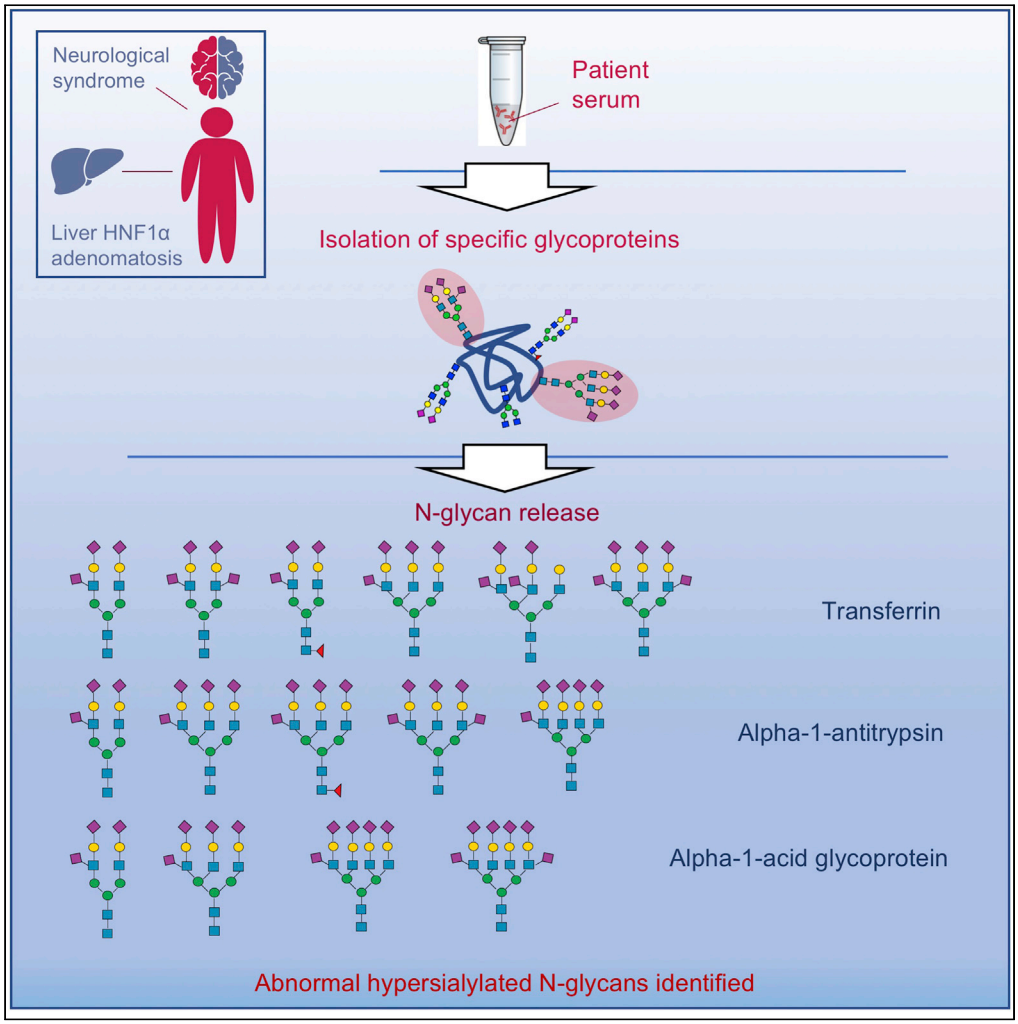

Luisa Sturiale, Marie-Cécile Nassogne, Angelo Palmigiano, ..., Rita Barone, Jaak Jaeken, Domenico Garozzo

domenico.garozzo@cnr.it

Highlights

Serum N-glycome is altered in a boy with neurological syndrome and *HNF1α* mutated HCA

Glycomics reveals unique hypersialylated N-glycans with two NeuAc per antenna

In-depth MS studies show the additional NeuAc is α2-6 linked to an outer arm GlcNAc

Sturiale et al., iScience 24, 102323
April 23, 2021, 2021 © 2021 The Author(s).
https://doi.org/10.1016/j.isci.2021.102323

iScience

CellPress
OPEN ACCESS

Article

Aberrant sialylation in a patient with a *HNF1α* variant and liver adenomatosis

Luisa Sturiale,[1] Marie-Cécile Nassogne,[2] Angelo Palmigiano,[1] Angela Messina,[1] Immacolata Speciale,[3,4] Rosangela Artuso,[5] Gaetano Bertino,[6] Nicole Revencu,[7] Xavier Stephénne,[8] Cristina De Castro,[4] Gert Matthijs,[9] Rita Barone,[1,10] Jaak Jaeken,[11] and Domenico Garozzo[1,12,*]

SUMMARY

Glycosylation is a fundamental post-translational modification of proteins that boosts their structural diversity providing subtle and specialized biological properties and functions. All those genetic diseases due to a defective glycan biosynthesis and attachment to the nascent glycoproteins fall within the wide area of congenital disorders of glycosylation (CDG), mostly causing multisystem involvement. In the present paper, we detailed the unique serum N-glycosylation of a CDG-candidate patient with an unexplained neurological phenotype and liver adenomatosis harboring a recurrent pathogenic *HNF1α* variant. Serum transferrin isoelectric focusing showed a surprising N-glycosylation pattern consisting on hyposialylation, as well as remarkable hypersialylation. Mass spectrometry-based glycomic analyses of individual serum glycoproteins enabled to unveil hypersialylated complex N-glycans comprising up to two sialic acids per antenna. Further advanced MS analysis showed the additional sialic acid is bonded through an α2-6 linkage to the peripheral N-acetylglucosamine residue.

INTRODUCTION

Glycosylation is the most common and versatile post-translational modification of proteins that enhances their structural complexity and fulfills functional and regulatory roles in physiological conditions (Varki and Gagneux, 2017; Reily et al., 2019). Glycosylation changes can be due to mutations affecting genes directly or indirectly involved in the biosynthesis and attachment of glycan moieties of glycoproteins and glycolipids, causing congenital disorders of glycosylation (CDG) (Ng and Freeze, 2018; Péanne et al., 2018). CDG comprise disorders of protein N-glycosylation (the largest group), of protein O-glycosylation, of combined protein N- and O-glycosylation, of lipid glycosylation, and of glycosylphosphatidylinositol-anchor synthesis (Jaeken and Péanne, 2017; Freeze et al., 2017). Since glycosylation occurs ubiquitously, CDG may affect all organs and systems. They show very different phenotypes varying from single organ to multisystem diseases, usually with prominent central nervous system involvement (Freeze et al., 2012; Barone et al., 2014).

Next-generation sequencing techniques have expanded the CDG field to gene defects not strictly associated with the glycosylation machinery (Hennet, 2012; Ng and Freeze, 2018). In a wider perspective, as glycosylation is not template-driven, it is not surprising that a variety of genetic and acquired factors may secondarily affect the cellular glycome, as described for a broad range of diseases including cancer (Fuster and Esko, 2005; Adamczyk et al., 2012), diabetes (Rudman et al., 2019), neurodegenerative disorders (Barone et al., 2012; Palmigiano et al., 2016; Kizuka et al., 2017; Russell et al., 2017), inflammatory disorders (Gornik and Lauc, 2008; Reily et al., 2019), or autoimmune diseases (Delves, 1998; Goulabchand et al., 2014). Finally, environmental factors may act on the glycosylation machinery through epigenetic modifications (DNA methylation, RNA-mediated silencing and chromatin modifications) that regulate expression of genes involved in glycosylation (Zoldos et al., 2010). In this context, mass spectrometry (MS) techniques have provided, over the years, a wide range of analytical methodologies for glycan structural characterization (Barone, et al., 2009; Dotz and Wuhrer, 2019).

[1]CNR, Institute for Polymers, Composites and Biomaterials, IPCB, 95126 Catania, Italy

[2]Pediatric Neurology Unit, Cliniques Universitaires Saint-Luc, Université Catholique de Louvain, 1200 Brussels, Belgium

[3]Department of Chemical Sciences, University of Naples Federico II, 80100 Naples, Italy

[4]Department of Agricultural Sciences, University of Naples Federico II, 80055 Portici, Italy

[5]Medical Genetics Unit, Meyer Children's University Hospital, 50100 Florence, Italy

[6]Hepatology Unit, A.O.U. Policlinico-Vittorio Emanuele, Department of Clinical and Experimental Medicine, University of Catania, 95100 Catania, Italy

[7]Center for Human Genetics, Cliniques Universitaires Saint-Luc, Université Catholique de Louvain, 1200 Brussels, Belgium

[8]Service de Gastro-Entérologie et Hépatologie Pédiatrique, Cliniques Universitaires Saint-Luc, Université Catholique de Louvain, 1200 Brussels, Belgium

[9]Department of Human Genetics, Laboratory for Molecular Diagnosis, KU Leuven, 3000 Leuven, Belgium

[10]Child Neurology and Psychiatry, Department of Clinical and Experimental Medicine, University of Catania, 95100 Catania, Italy

[11]Center for Metabolic Diseases, UZ and KU Leuven, 3000 Leuven, Belgium

[12]Lead contact

*Correspondence: domenico.garozzo@cnr.it

https://doi.org/10.1016/j.isci.2021.102323

In the present work, we adopted matrix-assisted laser desorption/ionization time-of-flight MS (MALDI TOF) MS and MALDI tandem time-of-flight (TOF/TOF) MS, in combination with ultra-high-performance liquid chromatography-electrospray MS (UHPLC-ESI MS), to characterize the glycophenotype of a boy with liver adenomatosis due to a known *HNF1α* variant. Besides a still unexplained neurological phenotype, he showed a remarkable serum transferrin (Tf) isoelectric focusing (IEF) pattern of hypersialylation. In-depth MS analyses showed distinct serum N-glycan features due to complex-type hypersialylated glycoforms with antennary disialo-epitopes that, to the best of our knowledge, have not yet been described in humans. In addition, we observed a significant decrease of fucosylated multi-branched N-glycans both in the total serum N-glycome and in individual serum glycoproteins, in line with the decreased antennary fucosylation associated with *HNF1α* mutations (Thanabalasingham et al., 2013; Rudman et al., 2019; Juszczak et al., 2019).

RESULTS

Patient report

This boy, now aged 17 years, was born after a normal term pregnancy from unrelated parents. He has two sisters. Weight at birth was 2890 g, length 49 cm, and head circumference 32.5 cm. The neonatal period was uneventful.

He shows psychomotor disability (walking without support at 2 years; first words at 2 years; at 14 years he counts to 10 and writes his forename), epilepsy (staring, starting at 5.5 years, controlled by valproate and levetiracetam, and now by valproate only), growth retardation (at 16 years 8 months height was 150 cm (- 3.9 SD), weight was 45 kg (- 2.7 SD), and head circumference 56 cm (- 0.2 SD) and mild dysmorphism (thick lips, tongue between the lips, still milk teeth present at 14 years, short fingers). Non-verbal IQ performed at the age of 7 years (Leiter-R) revealed mild intellectual disability (IQ of 67). Brain MRI showed a short corpus callosum with small spenium.

On occasion of abdominal ache, an ultrasound examination was performed showing liver adenomatosis. Subsequent analysis of *HNF1α* showed a heterozygous known pathogenic variant (c.872delC; p.Pro291GlnfsX51) (Kristinsson et al., 2001). Immunohistochemistry of a liver biopsy showed absence of HNF1α staining, suggesting a loss of the second *HNF1α* allele in liver. The c.872delC mutation is also present in the patient's mother and in one of his sisters. They both have MODY3 diabetes. The patient has no diabetes as yet.

Laboratory investigation before the results of the genetic analysis were known, showed a few abnormal results: neutrophils 1000/μL (nl range: 2000–3000), serum Tf 8.6 g/L (nl range: 2.0–3.6), des-gamma carboxyprothrombin 7693 mUA/mL (nl < 45), iron binding capacity 215 μM (nl 50–95), thyroid-stimulating hormone 6.1 mU/L (nl 0.7–5.3) with normal free T4, antithrombin >140% (nl 78–130), protein C 42% (nl 70–130). Coagulation factors IX and XI and protein S were normal. Total sialic acid in urine was mildly increased (634 μmol/g creatinine; nl 140–560) and free sialic acid was normal. Tf IEF showed a peculiar pattern with an increase of the 1-, 2-, 3-, 4-, 5-, 6-, and 7-sialoTf bands (Figure 1).

A capture panel for 79 CDG was normal. Whole-exome sequencing showed no clear-cut explanation neither for the neurological syndrome nor for the aberrant sialylation.

N- and O-glycosylation analyses

N-glycan characterization was performed by MALDI TOF MS of the whole serum N-glycome (see Figure S1) and of four serum glycoproteins: Tf, alpha-1-antitrypsin (AAT), alpha-1-acid glycoprotein (AGP) and immunoglobulin G (IgG). Abnormal sialylated structures were detected and further investigated by MALDI TOF/TOF MS/MS and by UHPLC ESI-MS. Moreover, a decrease of fucosylated tri-antennary N-glycans was detected in the MALDI TOF mass spectrum from the patient and from two other patients with a different *MODY 3* variant (Figure S2). Reduced outer arm fucose insertion is a known biochemical hallmark of gene *HNF1α* variants causing MODY3 (Thanabalasingham et al., 2013; Rudman et al., 2019; Juszczak et al., 2019).

MS analysis of serum apoC-III did not show mucin type O-glycosylation defects in the patient (data not shown) (Wopereis et al., 2003).

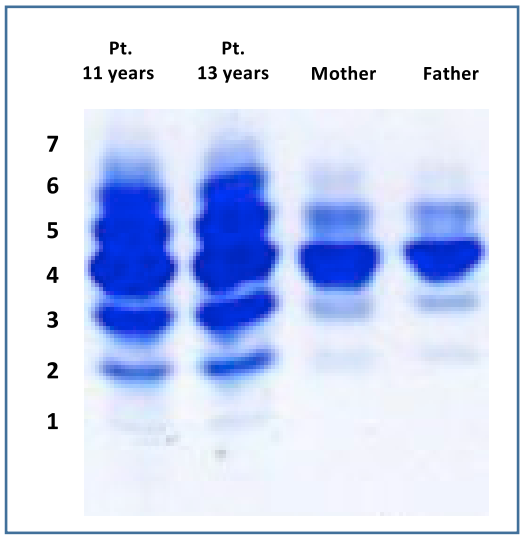

Figure 1. IEF profiles of serum Tf

IEF pattern of serum Tf from two patient serum samplings (at the age of 11 and 13 years), his mother and his father. Compared to the parents, taken as controls, the patient shows a marked increase of disialo-, trisialo-, pentasialo- and hexasialo-Tf isoforms, and traces of monosialo- and heptasialo-Tf bands.

Tf N-glycan analysis by MALDI TOF and MALDI TOF/TOF

Tf N-glycan MALDI-MS analysis on patient at age 11, revealed a unique profile (Figure 2A) with an intense additional peak at *m/z* 3153.4 attributable to a biantennary disialo-structure bearing a supplementary sialic acid residue. Likewise, less intense peaks were detected at *m/z* 3327.5, corresponding to its fucosylated counterpart, at *m/z* 3514.6, corresponding to a biantennary disialo-structure with two additional sialic acids and at *m/z* 3963.8, consistent with a triantennary tetrasialo-structure, as evidenced in Figure 2 inset. On the other hand, compared to a normal Tf N-glycan profile (Sturiale et al., 2011), a reduced intake of sialic acid on the glycan structures has been observed, as reflected by the increase of the biantennary monosialylated ion at *m/z* 2431.1 and of the mono- and disialo-triantennary ions at m/z 2880.3 and 3241.4, respectively.

MALDI TOF/TOF analyses on the two major abnormal glycoforms at *m/z* 3153.4 and *m/z* 3514.6 (Figures 2B and 2C) confirmed our attributions showing in the low mass-range three diagnostic fragments, such as the B-type ion at *m/z* 1208.5 ($NeuAc_2Gal_1GlcNAc_1$), the C-type ion at *m/z* 620.3 ($NeuAc_1Gal_1$) and the internal fragment (BZ ion, $NeuAc_1GlcNAc_1$) at *m/z* 611.3 (Domon and Costello, 1988; Spina et al., 2000), revealing the occurrence of a disialo-epitope bearing sialic acid linked either to galactose (Gal) and to N-acetylglucosamine (GlcNAc). The same ions were not found in the fragmentation pattern of the biantennary disialoglycan at *m/z* 2792.3, presenting an MS/MS spectrum in line with the canonical structure (data not shown).

As a whole, Tf N-glycan analyses reported in Figure 2, indicated the presence of abnormal biantennary structures capped with two sialic acids with an additional NeuAc unit at one or both the antennary GlcNAc residues.

Tf N-glycosylation analysis on a second patient serum aliquot, sampled at age 13 years, showed a further increase of these hypersialylated structures, as reported in Figure S3.

MALDI TOF and MALDI TOF/TOF N-glycan analysis on other serum glycoproteins

We also investigated the possible occurrence of this peculiar glycosylation on three other serum glycoproteins: AAT, AGP and IgG. Compared to Tf, these glycoproteins possess a more heterogeneous glycosylation. In particular, AAT and AGP exhibit a higher sialylation degree due to a greater amount of tri-, and tetra-branched fully sialylated N-glycan structures, potentially susceptible of further GlcNAc antennary sialylation.

AAT, one of the most abundant liver-derived serum glycoproteins, belongs to the superfamily of serine protease inhibitors (serpins). This acute phase protein plays an active anti-inflammatory role (McCarthy et al., 2014) and is a 52 kDa glycoprotein with three N-glycosylation sites at Asn70, Asn107, and Asn271, bearing di-, tri- or tetra-antennary glycans, as demonstrated by the MALDI TOF MS N-glycans profile of

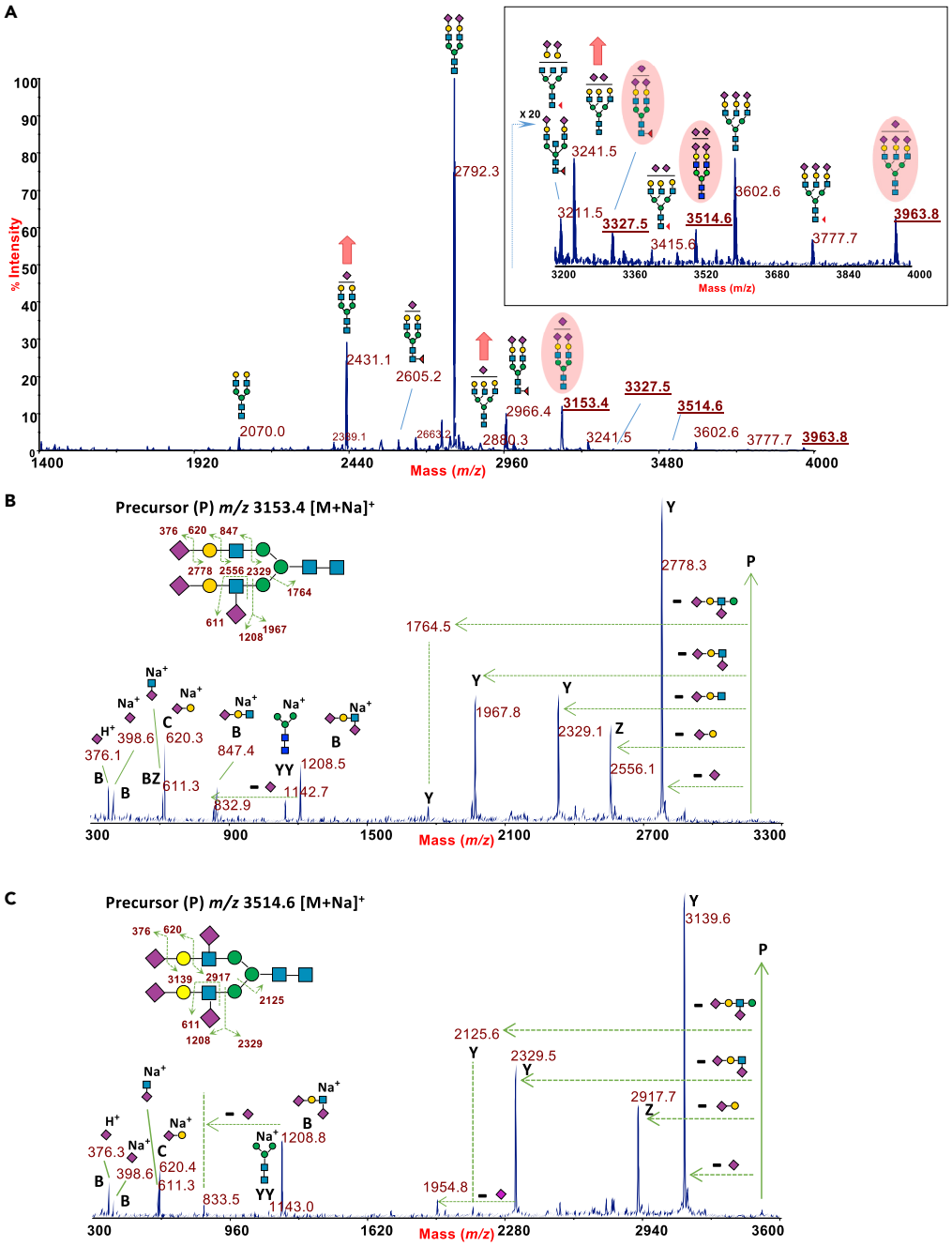

Figure 2. MALDI TOF MS analysis unveils the atypical sialylation of patient Tf N-glycans

(A) MALDI TOF mass spectrum of N-glycans from patient serum Tf (first sampling at age 11 years). Highlighted species refer to the abnormally hypersialylated glycans. Red arrows indicate the relative increase of some hyposialylated structures with respect to a control Tf (not shown). Figure inset shows the enlarged mass-range at *m/z* 3200–4000. Protein sample was isolated from serum by immunoaffinity depletion on anti-human Tf IgY-linked microbeads as described in the Transparent Methods section. Glycans released by PNGase F digestion where further purified and permethylated before MS analysis, conducted in reflector mode and in positive polarity. Molecular ions were finally detected as sodium adducts: $[M+Na]^+$. This glycan profile is representative of at least three independent acquisitions.

(B) MALDI TOF/TOF fragmentation analysis of the trisialo-biantennary glycan at *m/z* 3153.4 (precursor ion), showing the location of the additional sialic acid at one peripheral GlcNAc residue.

Figure 2. *Continued*
(C) MALDI TOF/TOF fragmentation analysis of the tetrasialo-biantennary N-glycan at *m/z* 3514.6 (precursor ion), showing the location of the two additional sialic acids at the peripheral GlcNAc residues.
Glycan structures were assigned following consortium for functional glycomics guidelines: N-acetylglucosamine, blue square; mannose, green circle; galactose, yellow circle; sialic acid, purple lozenge; fucose, red triangle.

control AAT in Figure S4A. MALDI TOF MS analysis of the patient AAT N-glycans showed a series of additional hypersialylated structures ranging between the biantennary trisialo-structure at *m/z* 3153.4 and the tetra-antennary pentasialo-structure at *m/z* 4774.1 (Figure S4B). A slight increase of hyposialylated structures at *m/z* 2431.1 and 3241.4, was also observed, together with a significant decrease of tri-antennary and tetra-antennary fucosylated glycans as a result of the HNF1A-MODY mutation (Juszczak et al., 2019).

AGP is another abundant acute phase serum glycoprotein mainly secreted by hepatocytes. It is involved in different physiological and pathological functions such as drug binding and regulation of immunological and inflammatory responses (Fernandes et al., 2015). Structurally, human AGP is a heavily glycosylated serum protein of molecular mass 41–43 kDa (ca. 45% glycan content) with five N-glycosylation sites at Asn15, Asn38, Asn54, Asn75, and Asn85, occupied in a heterogeneous manner by branched complex N-glycans, mostly tri- and tetra-antennary ones (Treuheit et al., 1992; Imre et al., 2005). Figure 3A reports the MALDI TOF MS N-glycan profile of AGP extracted from patient serum, compared to serum AGP from a control (Figure 3B). The patient spectrum showed an altered AGP glycosylation, reflecting the abnormal structural findings already observed for Tf and AAT. In AGP, the most abundant hypersialylated glycan structures were detected at *m/z* 3963.9 (triantennary tetrasialo-glycan) an at *m/z* 4774.3 (tetra-antennary pentasialo-glycan). Minor abnormal structures were found at *m/z* 3153.4 (biantennary trisialo-glycan) and at m/z 5135.6 (tetra-antennary hexasialo-glycan). Patient AGP N-glycan spectrum also showed a clear-cut increase of tri-antennary (*m/z* 2880.3 and 3241.5) and tetra-antennary (*m/z* 3690.7 and 4051.9) hyposialylated structures, as indicated in Figure 3A by red arrows. Finally, we observed, also in this specific glycoprotein, an evident decrease of fucosylated triantennary (*m/z* 3415.6 and *m/z* 3776.8) and tetra-antennary (*m/z* 4226.0, *m/z* 4587.2, and *m/z* 4761.3) glycoforms associated to the reduced amount of antennary fucosylation in MODY 3 patients (Juszczak et al., 2019). MALDI TOF/TOF analysis on parent ions at *m/z* 3963.9 and 5135.6 (see Figures 4A and 4B), confirmed the occurrence of the antennary disialo-epitope bearing sialic acid units linked at both Gal and GlcNAc residues. The fragmentation pattern of the species at *m/z* 3963.9 revealed the occurrence of a second isoform with a lactosamine terminal group at one antenna and two disialo-antennary groups, as depicted in Figure 4A.

IgG is the largest family of human antibodies and the major component of glycoproteins in serum, where it is secreted by plasma B cells. IgG is a key effector of the innate and adaptive immune system, playing a modulatory role mainly due to two N-glycan moieties linked to Asn297 at the constant region of the fragment crystallizable (Fc) domain (Hayes et al., 2014). Variable glycosylation (15–25% of the circulating IgG) could also be present on the antigen binding (Fab) domain (van de Bovenkamp et al., 2016). The MS profile of patient IgG N-glycans, reported in Figure S5A, was found in line with other reference MALDI mass spectra of permethylated IgG oligosaccharides (Wada et al., 2007; Sturiale et al., 2019) showing, in the high mass range, only minor amounts of biantennary disialylated glycans. In the same region of the spectrum, a faint trace of the trisialylated biantennary glycoform was detected (see Figure S5B). Due to the very small amount of this unique glyco-biomarker, we are not sure whether this is a significant finding.

Tf N-glycosylation analysis by UHPLC-ESI MS

UHPLC-ESI MS analysis on *Rapi*Fluor-MS (RFMS)-labeled N-glycans from patient Tf has been employed to get further structural insights on the abnormally glycosylated N-glycans (Messina et al., 2020; Sturiale et al., 2019; Palmigiano et al., 2018). Figure 5 shows the superimposed extracted ion chromatograms (EICs) of the biantennary disialo-, trisialo- and tetrasialo-glycans found in patient serum Tf. Aside the dominant species (red chromatogram) corresponding to the isomeric disialo-structures at *m/z* 1267.985 eluting at the same retention time of their analogs in control Tf (data not shown), we observed also additional glycans attributed to two trisialo-isomers at *m/z* 1413.534 (green chromatogram, 20-fold enhanced sensitivity) and one tetrasialo-biantennary structure at *m/z* 1559.081 (violet chromatogram, 200-fold enhanced sensitivity). This chromatographic method, based on hydrophilic interaction liquid chromatography (HILIC)-UPLC separation of RFMS labeled N-glycans, allows us to achieve well-resolved differentiations of sialo-linkage isomers, with the structures containing the highest number of α2-6 linked sialic acids more retained than the

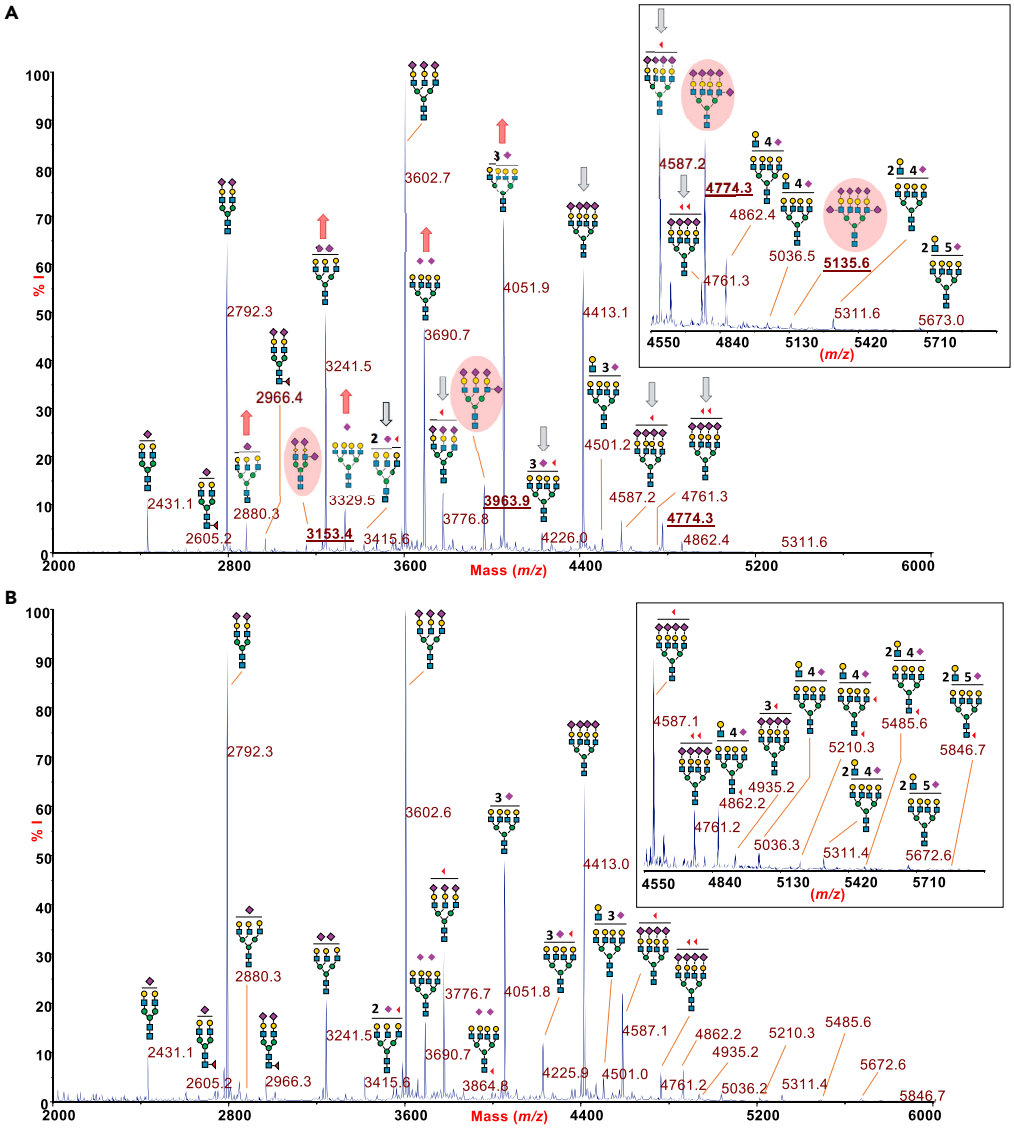

Figure 3. MALDI TOF MS analysis of patient serum AGP mapping sialylation changes of higher branched N-glycans

(A) MALDI TOF mass spectrum of N-glycans from patient serum AGP. Highlighted species refer to the abnormally hypersialylated species. Red arrows indicate the relative increase of some hyposialylated structures with respect to a control AGP from a healthy donor sample.

(B). Blue arrows indicate the relative decrease of the fully sialylated tri-antennary and tetra-antennary structures. Figure insets report the enlarged mass-range at *m/z* 4550–5900. Protein sample was isolated from serum by immunoaffinity depletion on anti-AGP IgY microbead spin columns as described in the Transparent Methods section. Glycans released by PNGase F digestion where further purified and permethylated before MS analysis, conducted in reflector mode and in positive polarity. Molecular ions were finally detected as sodium adducts: $[M+Na]^+$. This glycan profile is representative of at least three independent acquisitions. Glycan structures were assigned following consortium for functional glycomics guidelines: N-acetylglucosamine, blue square; mannose, green circle; galactose, yellow circle; sialic acid, purple lozenge.

α2-3-linked counterparts (Messina et al., 2020; Palmigiano et al., 2018; Palmisano et al., 2013). As a matter of fact, either the two isobaric N-linked biantennary disialo-glycans and the two trisialo-glycans eluted at distinct retention times, due to the occurrence of α2-6 or α2-3 sialyl-linkage types (Figure 5). To get possible assignments of the isomeric hypersialylated structures, we moreover compared the joint EICs of patient biantennary trisialo- and triantennary tetrasialo-glycans with the similar structures present in bovine fetuin

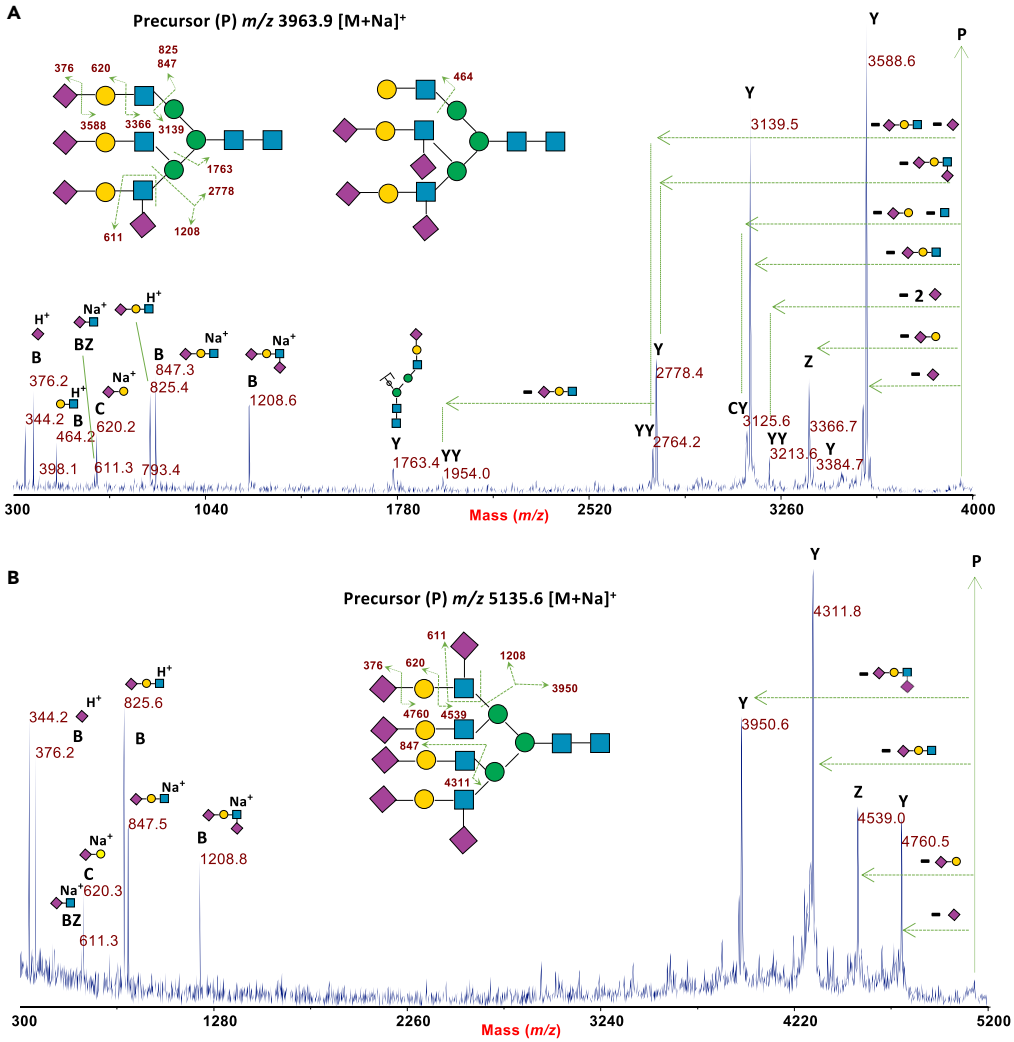

Figure 4. MALDI TOF/TOF analysis of highly branched hypersialylated AGP N-glycans allows to allocate the extra sialic acid at the peripheral GlcNAc

(A) MS/MS mapping of the tetrasialo-triantennary precursor (P) at m/z 3963.9.

(B) MS/MS mapping of the hexasialo-tetraantennary precursor (P) at *m/z* 5135.6. N-acetylglucosamine, blue square; mannose, green circle; galactose, yellow circle; sialic acid, purple lozenge.

(Figure 6), a widely studied protein bearing a good deal of N-glycans with the same composition of the patient atypical sialoglycans. In fact, fetuin from fetal calf serum mostly bears trisialo-triantennary complex glycans as major Asn-linked oligosaccharide component and a significant amount (about 8% of total N-glycans) of tribranched tetrasialo-structures. Previous studies (Green et al., 1988) identified two major isomeric tetrasialo-triantennary N-glycans in fetuin, accounting for 5.2% and 2.5% of the total N-glycan content, respectively. Both bear a disialo-antenna with a NeuAc moiety α2,6 linked to the peripheral GlcNAc and the other NeuAc unit attached through an α2,3 linkage to the Gal residue, indicated as structures IV and V in Figure 6A. These specific tetrasialo-isomers gave a couple of peaks eluting at 33.1 and 33.8 min in our UHPLC separation, as depicted in Figure 6B. The EIC obtained for the tetrasialo-triantennary N-glycans in patient Tf (Figure 6C) likewise showed two glycoforms sharing the same retention times with the corresponding isobaric species in fetuin, thus suggesting the occurrence of the same isomers in terms of α2-3 and α2-6 sialic acid number and location. Figure 6B also showed at lower retention times (28.5 and 29.5 min) two minor chromatographic peaks, corresponding to biantennary trisialo-structures. Basing on the observed retention times and on the knowledge of the sialo-linkage types of the biantennary structures recognized in bovine fetuin (Green et al., 1988), it could be reasonably assumed that these peaks

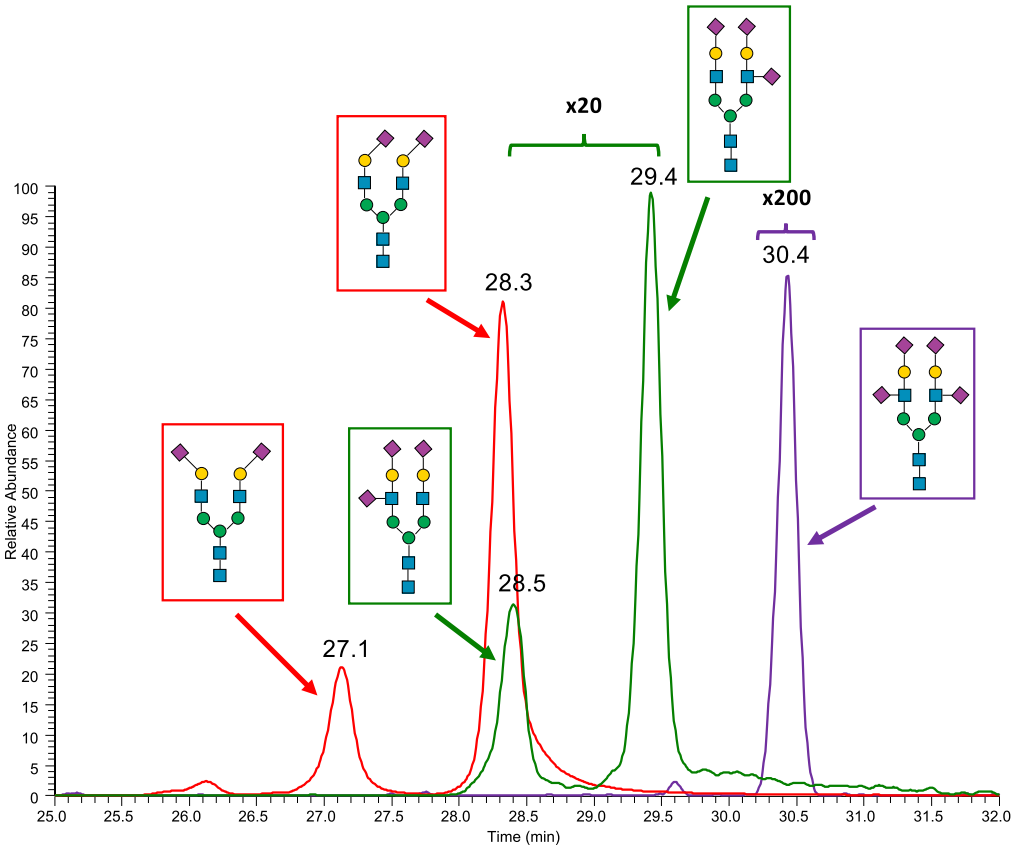

Figure 5. UHPLC-ESI MS analysis of disialo-, trisialo- and tetrasialo-biantennary N-glycans from patient serum Tf pinpoints different sialo-isomers

Superimposed extracted ion chromatograms (EICs) of some significant RFMS labeled Tf biantennary sialoglycans. Disialo-isomers (red chromatogram) and trisialo-isomers (green chromatogram) eluted at different retention times depending on α2-6 or α2-3 NeuAc linkage positions at the Gal residue. Ion currents associated to the tri-sialylated and tetra-sialylated species (violet chromatogram) are reported with 20-fold and 200-fold enhanced intensity, respectively. The PNGase released oligosaccharides were RFMS labeled and separated by HILIC as described in the Transparent Methods section. N-acetylglucosamine, blue square; mannose, green circle; galactose, yellow circle; sialic acid, purple lozenge (+ 45°: α2–6 linked; -45°: α2–3 linked; vertical and horizontal linkages: unassigned).

fit the glycan structures I, II, and III reported in Figure 6A, all containing the same disialo-structural motifs with one NeuAc unit α2-6 linked to the antennary GlcNAc and the other NeuAc residue α2-3 linked to Gal. Patient Tf chromatogram in Figure 6C, displayed, in its turn, two intense biantennary trisialo-ion signals at the same retention times of the corresponding species in bovine fetuin, suggesting the same sialic acid linkages on the disialo-branch.

DISCUSSION

The present study provides strong evidence for an aberrant sialylation of individual serum N-glycoforms in a patient with *HNF1α* mutated liver adenomatosis.

HNF1α is a homeobox transcription factor expressed in pancreatic isles, liver, kidney and intestine. Mono-allelic mutations of hepatocyte nuclear factor 1α (*HNF1α*) are identified in almost 30–50% of patients with maturity-onset diabetes of the young (MODY), so called MODY- subtype 3 (MODY 3). MODY is a rare condition, accounting for almost 1–5% of all cases of diabetes (Kim, 2015). In addition to MODY3, mutations of *HNF1α* may lead to hepatocellular adenomas and liver adenomatosis. Biallelic mutations of *HNF1α* are found in 30–35% of all hepatocellular adenomas (HNF1α-inactivated hepatocellular adenoma; HHCA). HNF1α acts as a master regulator of plasma protein antennary fucosylation by promoting both de novo

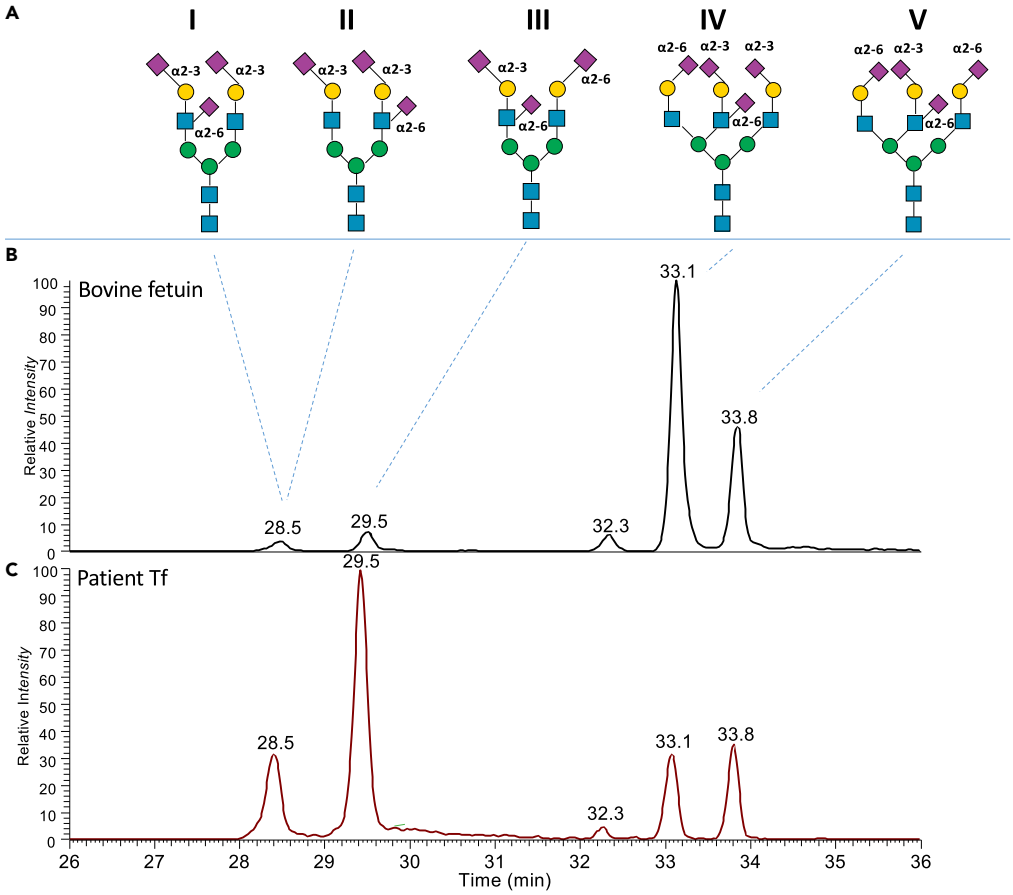

Figure 6. Direct comparison between UHPLC-ESI MS analysis of trisialo- and tetrasialo-glycans in patient Tf and bovine fetuin is suggestive of a common disialo-structural motif

(A) Structure assignments for RFMS labeled trisialo-biantennary and tetrasialo-triantennary N-glycan isomers in bovine fetuin and patient transferrin.

(B) EIC of the RFMS-labeled biantennary and triantennary hypersialylated structures in bovine fetuin.

(C) EIC of the RFMS-labeled biantennary and triantennary hypersialylated structures in patient Tf. The PNGase released oligosaccharides were RFMS-labeled and separated by HILIC as described in the Transparent Methods section.

N-acetylglucosamine, blue square; mannose, green circle; galactose, yellow circle; sialic acid, purple lozenge (+ 45°: α2–6 linked; -45°: α2–3 linked).

and the salvage pathways of GDP-fucose synthesis, stimulating the expression of FUT3, FUT5 and FUT6, and supressing the expression of FUT8 (Lauc et al., 2010). The present patient had c.872delC mutation in exon 4 of *HNF1α*, causing deletion of one of eight consecutive cytosine in a mutational hotspot of the gene resulting in frameshift and premature termination of the protein (Kristinsson et al., 2001). In the present patient liver adenomas were associated with loss of *HNF1α* expression in the hepatic tissue.

Unlike CDG and secondary disorders of hypoglycosylation (such as galactosemia and hereditary fructose intolerance) that are characterized by hyposialylation (Abu Bakar et al., 2018; Sturiale et al., 2005; Quintana et al., 2009), the present patient shows evident hypersialylation of the most abundant liver secreted serum glycoproteins, due to the occurrence of disialo-epitopes bearing one NeuAc α-2-3 linked to galactose (Gal) and the other NeuAc α2-6 linked to the peripheral N-acetylglucosamine (GlcNAc) residue.

Sialylation of the terminal end of glycans has an important role in signaling and adhesion processes at the bases of cell-cell recognition and cell-matrix interactions (Schnaar et al., 2014; Li and Ding, 2019). It provides negatively charged monosaccharide units to the carbohydrate determinants on the cellular surface. The α2-6 sialylation of a subterminal GlcNAc residue is a very uncommon feature in humans. It was found differentially expressed as ganglioside determinant in human colon cancer (Fukushi et al., 1986; Tsuchida

et al., 2003; Miyazaki et al., 2004), and as human milk oligosaccharide (HMO) component in monosialylated lacto-N-tetraose isomer b (LST b) and in disialyllacto-N-tetraose (DSLNT) (Bode, 2012), but, to the best of our knowledge, was not once described as a part of a disialo-terminal branch of human N-glycoproteins, as in the present patient. In other mammalian species, NeuAcα2-6GlcNAc N-glycan epitopes have been recognized since the 1980s in bovine and murine liver N-glycoproteins such as rat AGP, bovine prothrombin and bovine fetuin (Mizuochi et al., 1979; Yoshima et al., 1981; Green et al., 1988). In all the above reported structures (except in monosialo-oligomer LTS b), this disaccharide belongs to a disialylated NeuAcα2-3Galβ1-3(NeuAcα2-6)GlcNAc determinant. Six distinct ST6GalNAc are known to mediate the formation of α2-6 sialyl-linkages onto GalNAc residues of O-linked glycans and gangliosides in humans, but not a single ST6GlcNAc, catalyzing the transfer of sialic acid to the peripheral GlcNAc of N-glycans, has yet been identified, not even its substrate specificity. The product of such enzyme activity was found instead in murine tissues (Paulson et al., 1984; de Heij et al., 1986), as well as in bovine serum N-linked glycans (Mizuochi et al., 1979; Yoshima et al., 1981; Green et al., 1988). There is experimental evidence that ST6GalNAcV catalyzes the α2-6-sialylation of the GlcNAc in colon cancer cell lines in a highly ordered manner, as this reaction requires a trisaccharide containing an α2-3-sialylated Gal residue (Tsuchida et al., 2003), but all this issue remains not well defined.

No changes in the sialylation of liver derived glycoproteins have been reported in patients with monoallelic *HNF1α* mutations (Lauc et al., 2010). Accordingly, we did not find any significant change of the serum glycome in the patient's mother who carries the same *HNF1α* variant, in two subjects with MODY3-diabetes and *HNF1α* mutations nor in one patient with idiopathic liver adenomatosis (data not shown).

Selective expression of specific terminal glycosyltransferases is responsible for the synthesis of tissue-specific carbohydrate structures. Liver-enriched transcription factor hepatocyte nuclear factor-la regulates expression of glycosyltransferases implicated in sialylation of terminal N-glycan structures such as β-galactoside-α2,6-sialyltransferase in the liver (Svensson et al., 1992). It is conceivable that HNF1α-inactivated hepatocellular adenoma may be associated with modification of cell-type-specific transcription and expression of glycosyltransferases providing this unorthodox disialo-structures on liver derived N-glycoproteins. In favor of this association with liver adenomatosis is the fact that such disialyl-epitopes have been previously detected in human only in tumor tissues, as colon adenocarcinoma (Fukushi et al., 1986). Gene expression analyses might unravel differential expression of glycosyltransferases thus explaining the remarkable glycosylation pattern in the present patient with HNF1α-inactivated hepatocellular adenomas.

In conclusion, we report an aberrant N-glycosylation feature in a boy with unexplained psychomotor disability, epilepsy, mild dysmorphism, and with *HNF1α* mutated liver adenomas. Serum Tf IEF showed a pattern never seen before in our lab: an increase of all bands (1-sialo up to 7-sialo) except asialo-Tf, suggestive of hypersialylation. Mutation analysis revealed a pathogenic variant in the *HNF1α* gene (MODY3, explaining the liver adenomas). Glycomics MS investigation showed a decrease of fucosylated multibranched N-glycans both in the total serum N-glycome and in individual serum glycoproteins, consistent with the serum glycome profile of monoallelic *HNF1α* mutations. Most important, throughput MS investigations confirmed hypersialylation of serum Tf and other liver-derived serum glycoproteins and detected an abnormal sialylation bond that, as far as we know, has not been described in human N-glycoproteins.

Limitation of the study

One of the main difficulties when dealing with rare genetic disorders is their low prevalence that often limits the recruitment of additional patients to validate distinctive traits of the disease-related structural features at molecular level. This is particularly true for the present patient, showing an unexplained neurological syndrome, a pathogenic *HNF1α* variant and an extremely rare sialylation abnormality. The mechanism responsible for the hypersialylation with an abnormal sialylation bond in the present patient remains unclear.

Expression analyses of sialyltransferases and fucosyltransferases (i.e. *ST3GalIV*, *ST6GalI*, *FUT8* genes) may unravel, in the foreseeable future, the molecular mechanism underpinning patient's abnormal glycosylation pattern. Further studies may well consider to systematically evaluate serum N-glycosylation in patients with *HNF1α*-liver adenomatosis with special regard to hypersialylation features. Moreover, the occurrence of the neurological syndrome and possible links with abnormal sialylation in the present patient deserve further investigations.

Resource availability

Lead contact

Further information and requests for resources and reagents should be directed to and will be fulfilled by the lead contact, Domenico Garozzo (domenico.garozzo@cnr.it)

Materials availability

This study did not generate new unique reagents.

Data and code availability

This study did not generate datasets.

METHODS

All methods can be found in the accompanying transparent methods supplemental file.

SUPPLEMENTAL INFORMATION

Supplemental information can be found online at https://doi.org/10.1016/j.isci.2021.102323.

ACKNOWLEDGMENTS

This research was partially supported by ERA-Net for Research on Rare Diseases (ERA-NET Cofund action; FWO GOI2918N; EUROGLYCAN-omics) (GM, J.J.).

AUTHOR CONTRIBUTIONS

L.S., R.B., D.G., and J.J. wrote the manuscript. J.J., M.C.N., and X.S. performed clinical evaluation and follow-up of the principal patient. R.A., S.R.G., and G.B. performed clinical evaluation and genetic assessment of the patients involved in this study. N.R., G.M., R.A., and S.R.G. performed genetic analyses and results interpretation. R.B., R.A., and J.J. collected and compared the clinical data. L.S., A.P., A.M., I.S., C.D.C., and D.G. carried out the glycan analyses and the interpretation of the results. J.J. and R.B. provided additional intellectual input. L.S., D.G., and J.J. supervised research.

DECLARATION OF INTERESTS

The authors declare no competing interests.

Received: November 26, 2020
Revised: February 18, 2021
Accepted: March 15, 2021
Published: April 23, 2021

REFERENCES

Abu Bakar, N., Lefeber, D.J., and van Scherpenzeel, M. (2018). Clinical glycomics for the diagnosis of congenital disorders of glycosylation. J. Inherit. Metab. Dis. *41*, 499–513.

Adamczyk, B., Tharmalingam, T., and Rudd, P.M. (2012). Glycans as cancer biomarkers. Biochim. Biophys. Acta *1820*, 1347–1353.

Barone, R., Sturiale, L., and Garozzo, D. (2009). Mass spectrometry in the characterization of human genetic N-glycosylation defects. Mass Spectrom. Rev. *28*, 517–542.

Barone, R., Sturiale, L., Palmigiano, A., Zappia, M., and Garozzo, D. (2012). Glycomics of pediatric and adulthood diseases of the central nervous system. J. Proteomics *75*, 5123–5139.

Barone, R., Fiumara, A., and Jaeken, J. (2014). Congenital disorders of glycosylation with emphasis on cerebellar involvement. Semin. Neurol. *34*, 357–366.

Bode, L. (2012). Human milk oligosaccharides: every baby needs a sugar mama. Glycobiology *22*, 1147–1162.

de Heij, H.T., Koppen, P.L., and van den Eijnden, D.H. (1986). Biosynthesis of disialylated beta-D-galactopyranosyl-(1——3)-2-acetamido-2-deoxy-beta-D-glucopy ran osyl oligosaccharide chains. Identification of a beta-D-galactoside alpha-(2——3)- and a 2-acetamido-2-deoxy-beta-D-glucoside alpha-(2——6)-sialyltransferase in regenerating rat liver and other tissues. Carbohydr. Res. *149*, 85–99.

Delves, P.J. (1998). The role of glycosylation in autoimmune disease. Autoimmunity *27*, 239–253.

Domon, B., and Costello, C.E. (1988). A systematic nomenclature for carbohydrate fragmentations in FAB-MS/MS spectra of glycoconjugates. Glycoconj. J. *5*, 397–409.

Dotz, V., and Wuhrer, M. (2019). N-glycome signatures in human plasma: associations with physiology and major diseases. FEBS Lett. *593*, 2966–2976.

Fernandes, C.L., Ligabue-Braun, R., and Verli, H. (2015). Structural glycobiology of human α1-acid glycoprotein and its implications for pharmacokinetics and inflammation. Glycobiology *25*, 1125–1133.

Freeze, H.H., Eklund, E.A., Ng, B.G., and Patterson, M.C. (2012). Neurology of inherited glycosylation disorders. Lancet Neurol. *11*, 453–466.

Freeze, H.H., Schachter, H., and Kinoshita, T. (2017). Genetic disorders of glycosylation. In Essentials of Glycobiology, Third Edition, A. Varki, R.D. Cummings, J.D. Esko, P. Stanley, G.W. Hart, M. Aebi, A.G. Darvill, T. Kinoshita, N.H. Packer, and J.H. Prestegard, et al., eds. (Cold Spring Harbor Laboratory Press), pp. 2015–2017.

Fukushi, Y., Nudelman, E., Levery, S.B., Higuchi, T., and Hakomori, S. (1986). A novel disialoganglioside ($IV^3NeuAcII^6NeuAcLc_4$) of human adenocarcinoma and the Monoclonal Antibody (FH9) defining this disialosyl structure. Biochemistry *25*, 2859–2866.

Fuster, M.M., and Esko, J.D. (2005). The sweet and sour of cancer: glycans as novel therapeutic targets. Nat. Rev. Cancer *5*, 526–542.

Gornik, O., and Lauc, G. (2008). Glycosylation of serum proteins in inflammatory diseases. Dis. Markers. *25*, 267–278.

Goulabchand, R., Vincent, T., Batteux, F., Eliaou, J.F., and Guilpain, P. (2014). Impact of autoantibody glycosylation in autoimmune diseases. Autoimmun. Rev. *13*, 742–750.

Green, E.D., Adelt, G., Baenziger, J.U., Wilson, S., and Van Halbeek, H. (1988). The asparagine-linked oligosaccharides on bovine fetuin. Structural analysis of N-glycanase-released oligosaccharides by 500-megahertz 1H NMR spectroscopy. J. Biol. Chem. *263*, 18253–18268.

Hayes, J.M., Cosgrave, E.F., Struwe, W.B., Wormald, M., Davey, G.P., Jefferis, R., and Rudd, P.M. (2014). Glycosylation and fc receptors. Curr. Top. Microbiol. Immunol. *382*, 165–199.

Hennet, T. (2012). Diseases of glycosylation beyond classical congenital disorders of glycosylation. Biochim. Biophys. Acta *1820*, 1306–1317.

Imre, T., Schlosser, G., Pocsfalvi, G., Siciliano, R., Molnár-Szöllosi, E., Kremmer, T., Malorni, A., and Vékey, K. (2005). Glycosylation site analysis of human alpha-1-acid glycoprotein (AGP) by capillary liquid chromatography-electrospray mass spectrometry. J. Mass Spectrom. *40*, 1472–1483.

Jaeken, J., and Péanne, R. (2017). What is new in CDG? J. Inherit. Metab. Dis. *40*, 569–586.

Juszczak, A., Pavić, T., Vučković, F., Bennett, A.J., Shah, N., Pape Medvidov, E., Groves, C.J., Šekerija, M., Chandler, K., Burrows, C., et al. (2019). Plasma fucosylated glycans and C-reactive protein as biomarkers of HNF1A-MODY in young adult-onset nonautoimmune diabetes. Diabetes Care *42*, 17–26.

Kim, S.H. (2015). Maturity-onset diabetes of the young: what do clinicians need to know? Diabetes Metab. J. *39*, 468–477.

Kizuka, Y., Kitazume, S., and Taniguchi, N. (2017). N-glycan and Alzheimer's disease. Biochim. Biophys. Acta *1861*, 2447–2454.

Kristinsson, S.Y., Thorolfsdottir, E.T., Talseth, B., Steingrimsson, E., Thorsson, A.V., Helgason, T., Hreidarsson, A.B., and Arngrimsson, R. (2001). MODY in Iceland is associated with mutations in HNF-1α and a novel mutation in *NeuroD1*. Diabetologia *44*, 2098–2103.

Lauc, G., Essafi, A., Huffman, J.E., Hayward, C., Knežević, A., Kattla, J.J., Polašek, O., Gornik, O., Vitart, V., Abrahams, J.L., et al. (2010). Genomics meets glycomics-the first GWAS study of human N-Glycome identifies HNF1α as a master regulator of plasma protein fucosylation. PLoS Genet. *6*, e1001256.

Li, F., and Ding, J. (2019). Sialylation is involved in cell fate decision during development, reprogramming and cancer progression. Protein Cell *10*, 550–565.

McCarthy, C., Saldova, R., Wormald, M.R., Rudd, P.M., McElvaney, N.G., and Reeves, E.P. (2014). The role and importance of glycosylation of acute phase proteins with focus on alpha-1 antitrypsin in acute and chronic inflammatory conditions. J. Proteome Res. *13*, 3131–3143.

Messina, A., Palmigiano, A., Esposito, F., Fiumara, A., Bordugo, A., Barone, R., Sturiale, L., Jaeken, J., and Garozzo, D. (2020). HILIC-UPLC-MS for high throughput and isomeric N-glycan separation and characterization in Congenital Disorders Glycosylation and human diseases. Glicoconj. J. https://doi.org/10.1007/s10719-020-09947-7.

Miyazaki, K., Ohmori, K., Izawa, M., Koike, T., Kumamoto, K., Furukawa, K., Ando, T., Kiso, M., Yamaji, T., Hashimoto, Y., et al. (2004). Loss of disialyl Lewis(a), the ligand for lymphocyte inhibitory receptor sialic acid-binding immunoglobulin-like lectin-7 (Siglec-7) associated with increased sialyl Lewis(a) expression on human colon cancers. Cancer Res. *64*, 4498–4505.

Mizuochi, T., Yamashita, K., Fujikawa, K., Kisiel, W., and Kobata, A. (1979). The carbohydrate of bovine prothrombin. Occurrence of Gal beta 1 leads to 3GlcNAc grouping in asparagine-linked sugar chains. J. Biol. Chem. *254*, 6419–6425.

Ng, B.G., and Freeze, H.H. (2018). Perspectives on glycosylation and its congenital disorders. Trends Genet. *34*, 466–476.

Palmigiano, A., Barone, R., Sturiale, L., Sanfilippo, C., Bua, R.O., Romeo, D.A., Messina, A., Capuana, M.L., Maci, T., Le Pira, F., et al. (2016). CSF N-glycoproteomics for early diagnosis in Alzheimer's disease. J. Proteomics *131*, 29–37.

Palmigiano, A., Messina, A., Sturiale, L., and Garozzo, D. (2018). Advanced LC-MS methods for N-glycan characterization. In Comprehensive Analytical Chemistry Advances in the Use of Liquid Chromatography Mass Spectrometry (LCMS): Instrumentation Developments and Applications, *79*, A. Cappiello and P. Palma, eds. (Elsevier B.V), pp. 147–172.

Palmisano, G., Larsen, M.R., Packer, N.H., and Thaysen-Andersen, M. (2013). Structural analysis of glycoprotein sialylation–part II: LC-MS based detection. RSC Adv. *3*, 22706–22726.

Paulson, J.C., Weinstein, J., and de Souza-e-Silva, U. (1984). Biosynthesis of a disialylated sequence in N-linked oligosaccharides: identification of an N-acetylglucosaminide (alpha 2-6)-sialyltransferase in Golgi apparatus from rat liver. Eur. J. Biochem. *140*, 523–530.

Péanne, R., de Lonlay, P., Foulquier, F., Kornak, U., Lefeber, D.J., Morava, E., Pérez, B., Seta, N., Thiel, C., Van Schaftingen, E., et al. (2018). Congenital disorders of glycosylation (CDG): quo vadis? Eur. J. Med. Genet. *61*, 643–663.

Quintana, E., Sturiale, L., Montero, R., Andrade, F., Fernandez, C., Couce, M.L., Barone, R., Aldamiz-Echevarria, L., Ribes, A., Artuch, R., and Briones, P. (2009). Secondary disorders of glycosylation in inborn errors of fructose metabolism. J. Inherit. Metab. Dis. *32*, S273–S278.

Reily, C., Stewart, T.J., Renfrow, M.B., and Novak, J. (2019). Glycosylation in health and disease. Nat. Rev. Nephrol. *15*, 346–366.

Rudman, N., Gornik, O., and Lauc, G. (2019). Altered N-glycosylation profiles as potential biomarkers and drug targets in diabetes. FEBS Lett. *593*, 1598–1615.

Russell, A.C., Šimurina, M., Garcia, M.T., Novokmet, M., Wang, Y., Rudan, I., Campbell, H., Lauc, G., Thomas, M.G., and Wang, W. (2017). The N-glycosylation of immunoglobulin G as a novel biomarker of Parkinson's disease. Glycobiology *27*, 501–510.

Schnaar, R.L., Gerardy-Schahn, R., and Hildebrandt, H. (2014). Sialic acids in the brain: gangliosides and polysialic acid in nervous system development, stability, disease, and regeneration. Physiol. Rev. *94*, 461–518.

Spina, E., Cozzolino, R., Ryan, E., and Garozzo, D. (2000). Sequencing of oligosaccharides by collision-induced dissociation matrix-assisted laser desorption/ionization mass spectrometry. J. Mass Spectrom. *35*, 1042–1048.

Sturiale, L., Barone, R., Fiumara, A., Perez, M., Zaffanello, M., Sorge, G., Pavone, L., Tortorelli, S., O'Brien, J.F., Jaeken, J., and Garozzo, D. (2005). Hypoglycosylation with increased fucosylation and branching of serum transferrin N-glycans in untreated galactosemia. Glycobiology *15*, 1268–1276.

Sturiale, L., Barone, R., and Garozzo, D. (2011). The impact of mass spectrometry in the diagnosis of congenital disorders of glycosylation. J. Inherit. Metab. Dis. *34*, 891–899.

Sturiale, L., Bianca, S., Garozzo, D., Terracciano, A., Agolini, E., Messina, A., Palmigiano, A., Esposito, F., Barone, C., Novelli, A., et al. (2019). ALG12-CDG: novel glycophenotype insights endorse the molecular defect. Glycoconj. J. *36*, 461–472.

Svensson, E.C., Conley, P.B., and Paulson, J.C. (1992). Regulated expression of alpha 2, 6-sialyltransferase by the liver-enriched transcription factors HNF-1, DBP, and LAP. J. Biol. Chem. *267*, 3466–3472.

Thanabalasingham, G., Huffman, J.E., Kattla, J.J., Novokmet, M., Rudan, I., Gloyn, A.L., Hayward, C., Adamczyk, B., Reynolds, R.M., Muzinic, A., et al. (2013). Mutations in HNF1A result in marked alterations of plasma glycan profile. Diabetes *62*, 1329–1337.

Treuheit, M.J., Costello, C.E., and Halsall, H.B. (1992). Analysis of the five glycosylation sites of human alpha 1-acid glycoprotein. Biochem. J. *283*, 105–112.

Tsuchida, A., Okajima, T., Furukawa, K., Ando, T., Ishida, H., Yoshida, A., Nakamura, Y., Kannagi, R., Kiso, M., and Furukawa, K. (2003). Synthesis of

disialyl Lewis a (Le(a)) structure in colon cancer cell lines by a sialyltransferase, ST6GalNAc VI, responsible for the synthesis of alpha-series gangliosides. J. Biol. Chem. *278*, 22787–22794.

van de Bovenkamp, F.S., Hafkenscheid, L., Rispens, T., and Rombouts, Y. (2016). The emerging importance of IgG fab glycosylation in immunity. J. Immunol. *196*, 1435–1441.

Varki, A., and Gagneux, P. (2017). Biological functions of glycans. In Essentials of Glycobiology, Third Edition, A. Varki, R.D. Cummings, J.D. Esko, P. Stanley, G.W. Hart, M. Aebi, A.G. Darvill, T. Kinoshita, N.H. Packer, and J.H. Prestegard, et al., eds. (Cold Spring Harbor Laboratory Press), pp. 2015–2017.

Wada, Y., Azadi, P., Costello, C.E., Dell, A., Dwek, R.A., Geyer, H., Geyer, R., Kakehi, K., Karlsson, N.G., Kato, K., et al. (2007). Comparison of the methods for profiling glycoprotein glycans–HUPO Human Disease Glycomics/Proteome Initiative multi-institutional study. Glycobiology *17*, 411–422.

Wopereis, S., Grünewald, S., Morava, E., Penzien, J.M., Briones, P., García-Silva, M.T., Demacker, P.N., Huijben, K.M., and Wevers, R.A. (2003). Apolipoprotein C-III isofocusing in the diagnosis of genetic defects in O-glycan biosynthesis. Clin. Chem. *49*, 1839–1845.

Yoshima, H., Matsumoto, A., Mizuochi, T., Kawasaki, T., and Kobata, A. (1981). Comparative study of the carbohydrate moieties of rat and human plasma alpha 1-acid glycoproteins. J. Biol. Chem. *256*, 8476–8484.

Zoldoš, V., Grgurević, S., and Lauc, G. (2010). Epigenetic regulation of protein glycosylation. Biomol. Concepts *1*, 253–261.

iScience, Volume *24*

Supplemental information

Aberrant sialylation in a patient with a *HNF1α* variant and liver adenomatosis

Luisa Sturiale, Marie-Cécile Nassogne, Angelo Palmigiano, Angela Messina, Immacolata Speciale, Rosangela Artuso, Gaetano Bertino, Nicole Revencu, Xavier Stephénne, Cristina De Castro, Gert Matthijs, Rita Barone, Jaak Jaeken, and Domenico Garozzo

Supplemental Information

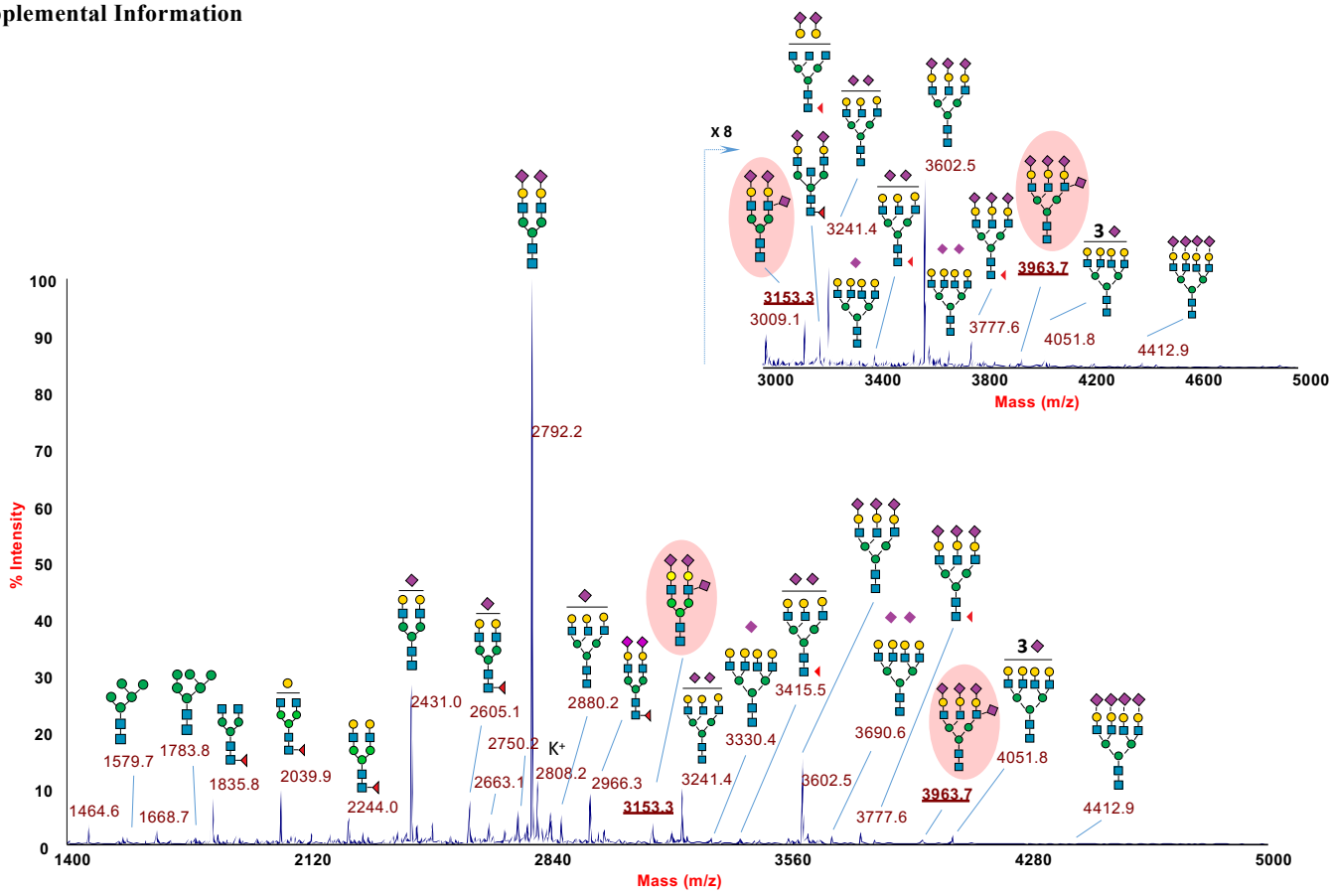

Figure S1. Related to Figures 2 and 3. MALDI-TOF MS profile of N-linked glycans from the whole patient serum glycoproteins.
Total patient serum N-glycome shows the occurrence of two of the most abundant peculiar glycoforms, namely the biantennary trisialo- and the triantennary tetrasialo-structure, both comprised in the mass-range between *m/z* 3000 and *m/z* 4000 (see inset). Figure inset reports the enlarged mass-range at *m/z* 3200–4000. Glycans were released from serum proteins as described in the Transparent Methods section. MS analysis were conducted on permethylated oligosaccharides in reflector mode and in positive polarity. Molecular ions were finally detected as sodium adducts: $[M+Na]^+$. This glycan profile is representative of at least three independent acquisitions.
N-acetylglucosamine, blue square; mannose, green circle; galactose, yellow circle; sialic acid, purple lozenge; fucose, red triangle.

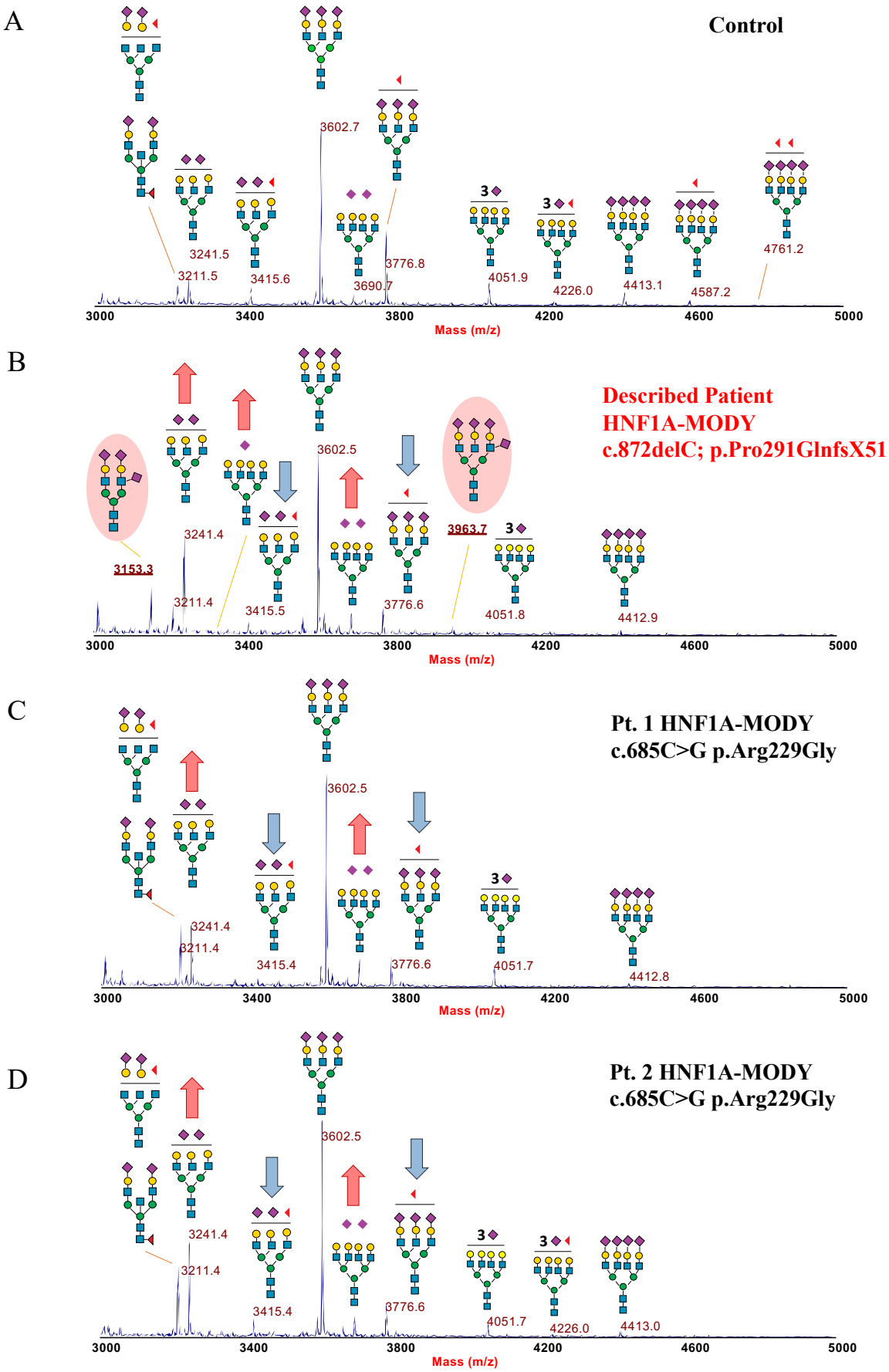

Figure S2. Related to Figure 3. MALDI-TOF mass spectra at high mass-range (*m/z* 3000-5000) of permethylated serum N-glycans from a control (A), the described patient (B) and two MODY patients with a different *HNF1A* variant (C, D).

This direct comparison allows to pinpoint, beside the typical patient sialo-biomarkers, also changes in the relative abundance of some triantennary species, such as the decrease of fucosylated glycans at *m/z* 3776.6 and, in minor extent, at *m/z* 3415.4, likely due to a decreased antennary fucosylation, which is the biochemical hallmark of HNF1A-MODY (Juszczak et al., 2019).

N-acetylglucosamine, blue square; mannose, green circle; galactose, yellow circle; sialic acid, purple lozenge; fucose, red triangle.

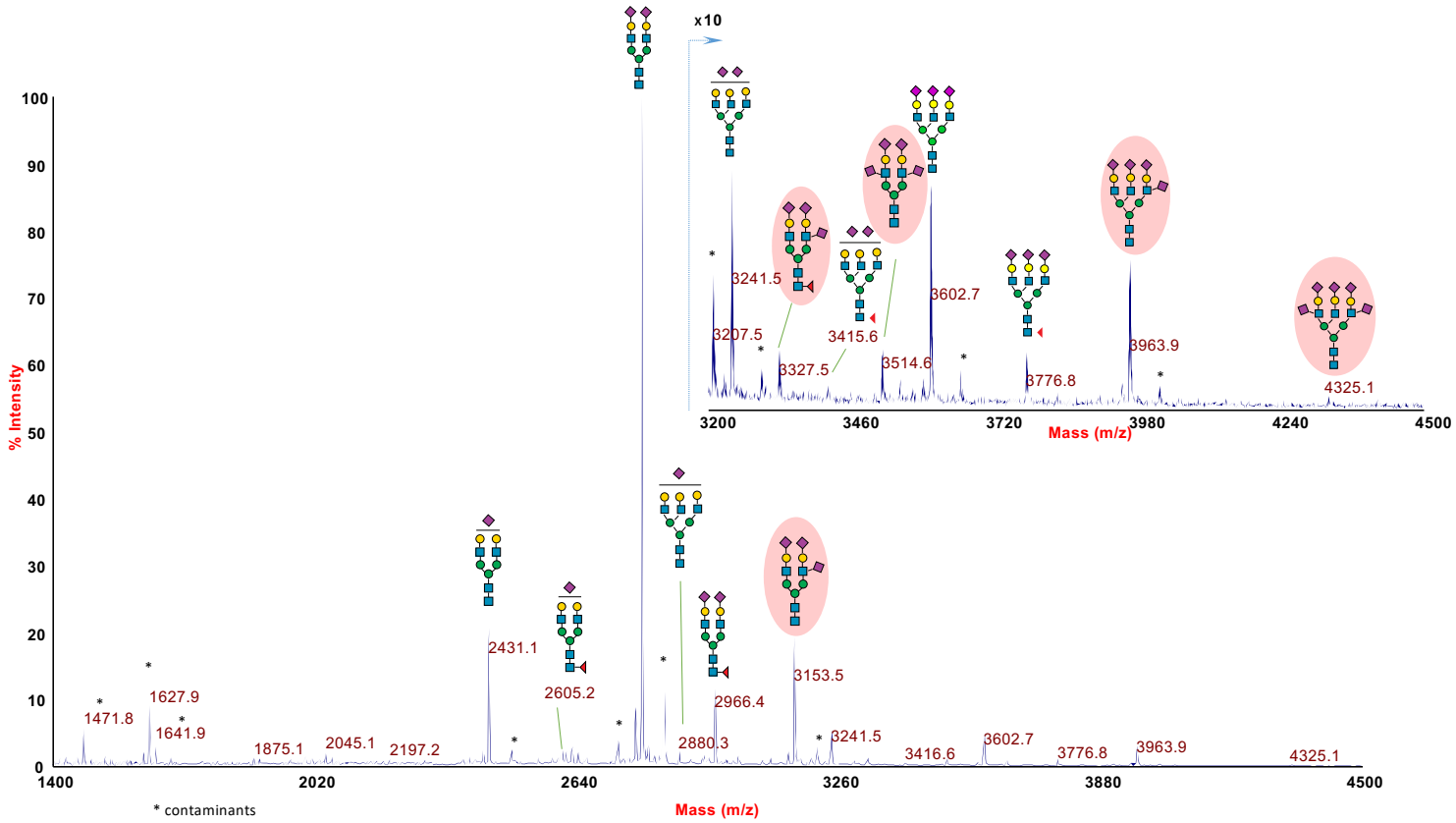

Figure S3. Related to Figure 2. MALDI TOF mass spectrum of N-glycans from patient serum Tf (second sample at age 13).
Compared to the first serum sampling at age 11, current Tf profile shows even more increased amounts of hypersialylated species, up to *m/z* 4325.1 (triantennary pentasialo-glycan).
N-acetylglucosamine, blue square; mannose, green circle; galactose, yellow circle; sialic acid, purple lozenge; fucose, red triangle.

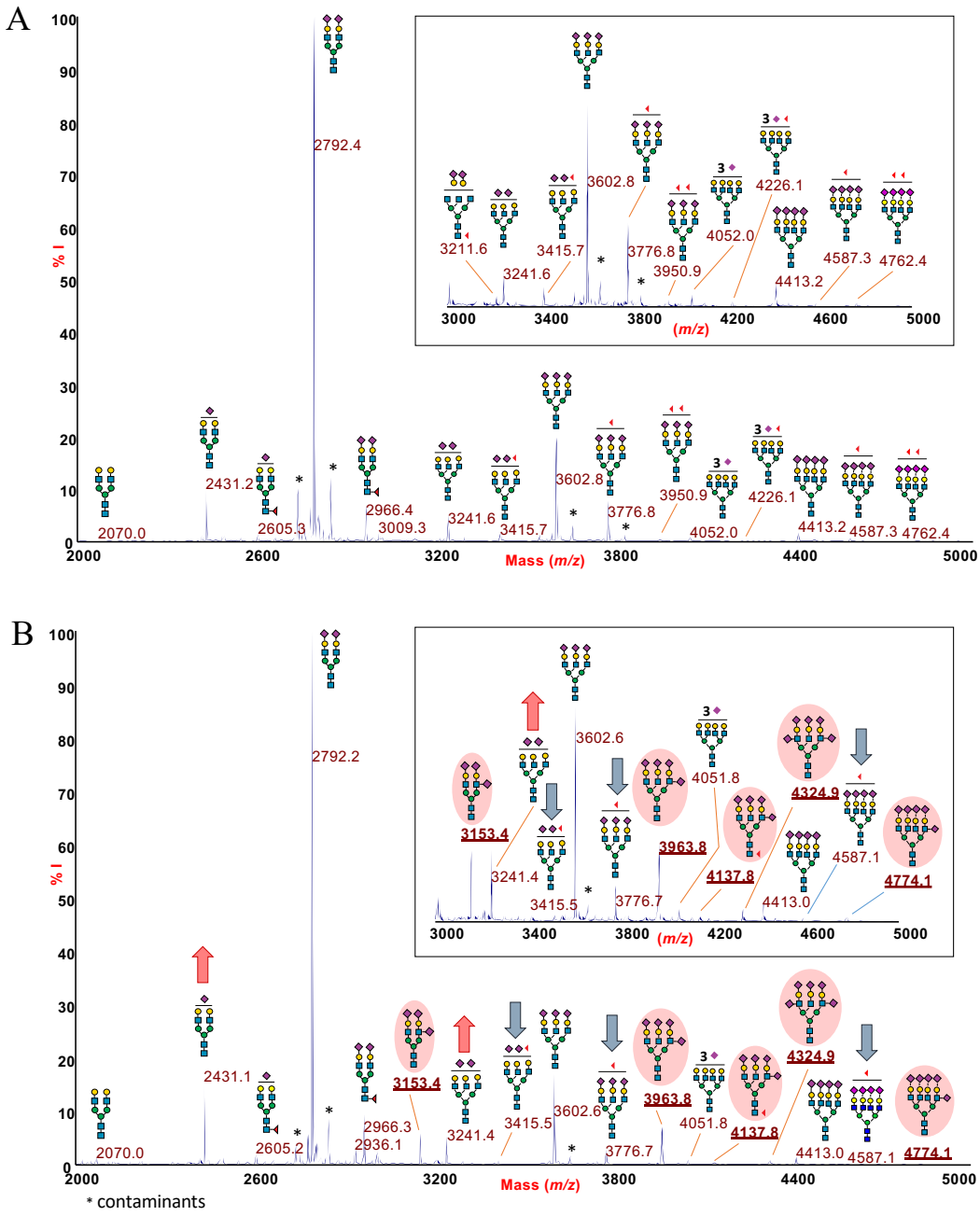

Figure S4. Related to Figure 2 and 3. Comparison of MALDI TOF MS profiles of N-glycans released from Control and Patient serum AAT.
(A) Control serum ATT. (B) Patient serum AAT. Figure insets report the enlarged mass-range at *m/z* 3000-5000.
The N-linked glycan repertoire of serum AAT is richer in tri- and tetra-antennary glycans than Tf, allowing us to detect in patient's sample up to five hypersialylated species (highlighted glycans). Additional glycosylation changes consist on the increase of hyposialylated glycans (red arrows). Decreased amounts of fucosylated tri-and tetra-antennary glycans were moreover detected (blue arrows), as previously reported for HNF1A-MODY patients (Juszczak et al., 2019). Protein sample was isolated from serum by immunoaffinity depletion on anti-AAT IgY microbead spin columns as described in the Transparent Methods section. Glycans released by PNGase F digestion where further purified and permethylated before MS analysis, conducted in reflector mode and in positive polarity. Molecular ions were finally detected as sodium adducts: $[M+Na]^+$. This glycan profile is representative of at least three independent acquisitions.
N-acetylglucosamine, blue square; mannose, green circle; galactose, yellow circle; sialic acid, purple lozenge; fucose, red triangle.

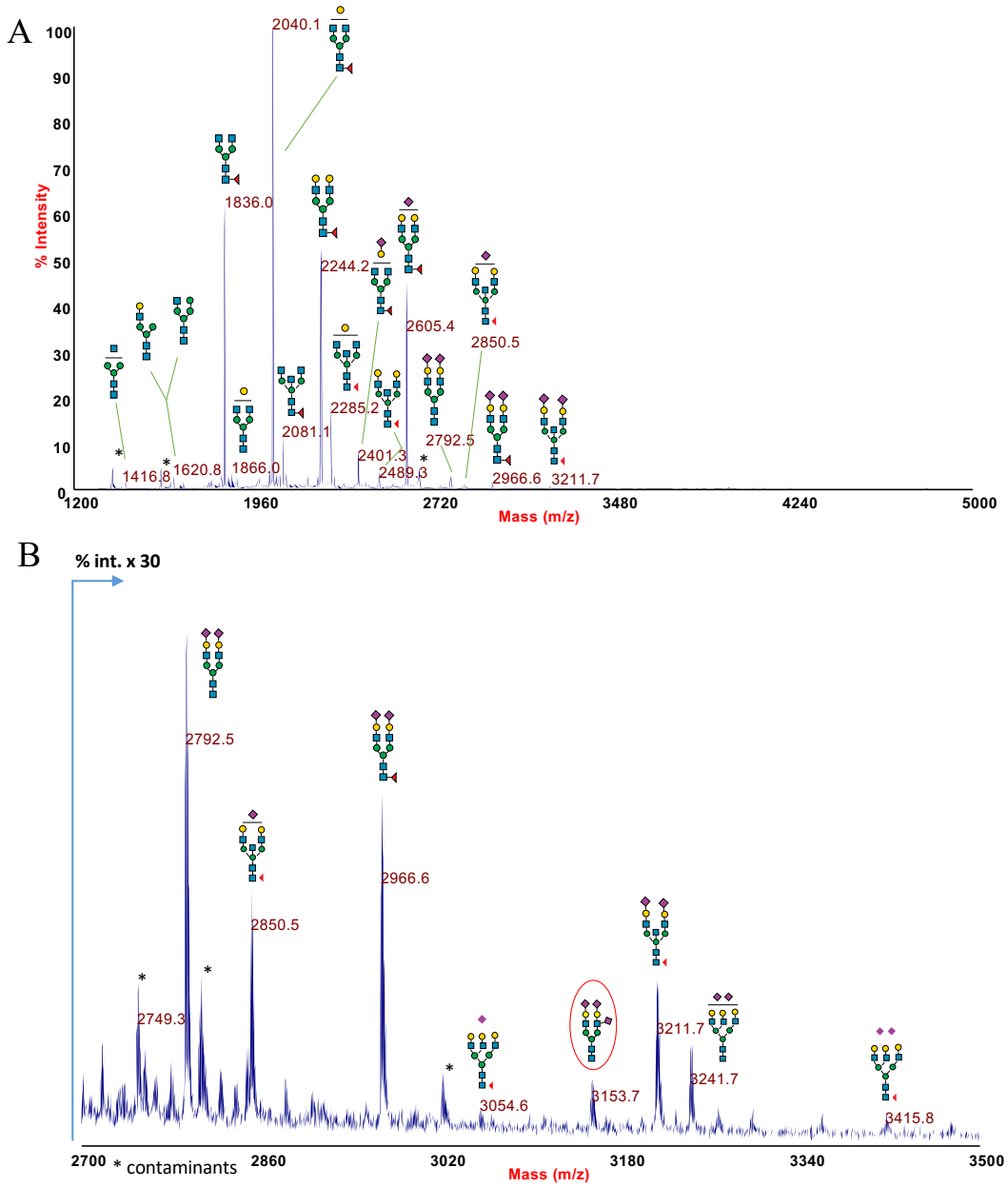

Figure S5. Related to Figure 2 and 3. MALDI TOF mass spectrum of N-glycans from patient serum IgG.
(A) Full-range MALDI-MS profile of patient IgG N-glycans. It was found in line with other reference MALDI mass spectra of permethylated IgG oligosaccharides (Wada et al., 2007; Sturiale et al., 2019) with four major peaks corresponding to fucosylated biantennary N-glycans bearing 0, 1 and 2 galactose residues (at *m/z* 1836.0, 2040.1 and 2244.2, respectively) and a monosialo- digalactosylated structure (at *m/z* 2605.4). Less intense peaks refer to fucosylated biantennary glycans with bisecting GlcNAc and variable galactosylation degree.
(B) Enlarged high mass-range (*m/z* 2700-3500), showing traces of minor glycan species as disialo-glycans together with a faint trace of the abnormal trisialo-biantennary glycoform at *m/z* 3153.7.
Protein sample was isolated from serum by immunoaffinity depletion on anti-IgG IgY microbead spin columns as described in the Transparent Methods section. Glycans released by PNGase F digestion where further purified and permethylated before MS analysis, conducted in reflector mode and in positive polarity. Molecular ions were finally detected as sodium adducts: $[M+Na]^+$. This glycan profile is representative of at least three independent acquisitions.
N-acetylglucosamine, blue square; mannose, green circle; galactose, yellow circle; sialic acid, purple lozenge; fucose, red triangle.

Transparent Methods

Ethical approval

All the described procedures involving human participants were in accordance with the protocols approved by the Ethical Committee of each institutional research center involved in this study, and with the Helsinki declaration. The patients detailed in this study provided informed consent.

Genetic analyses

Sanger sequencing was performed of the 9 coding exons and flanking intronic sequences of the *HNF1A* gene (NCBI reference sequence: NM_000545.8).

Tf glycosylation analysis by isoelectric focusing (IEF)

This analysis was performed as described (Van Eijk et al., 1983).

Glycoproteins purification from serum samples

Each individual serum glycoprotein was sequentially extracted from serum by immunoaffinity chromatography on microbeads derivatized with chicken polyclonal antibody (IgY) against human transferrin (Tf), human IgG, human alpa-1-antitripsin (ATT), and human acid-1-glycoprotein (AGP) respectively, as previously described (Sturiale et al. 2008). 120 µL of serum were diluted 1:5 in 10 mM Tris-Buffered Saline (TBS) pH 7.4 and loaded into spin columns pre-packed with 1 mL of specific IgY-derivatized stationary phases (Genway Biotech Inc.). After incubation (at RT for 15 min) and centrifugation (at 1000 x *g* for 30 sec), each column was washed three times with TBS to remove residual unbound proteins and finally subjected twice to a stripping step with 0.5 mL 0.1 M Glicine-HCl pH 2.5. Protein samples were then neutralized with 1M TBS pH 8.0 and concentrated up to about 100 µL in 50mM ammonium bicarbonate (NH_4HCO_3) pH 7.8 by Amicon® 30K Ultra-4 centrifugal filter devices (Merck, KGaA, Darmstadt, Germany). The described protocol is suitable to multiple serum protein extractions as follows: the protein-depleted serum and the washing solutions, containing the unretained IgY fractions, were in their turn pooled and concentrated with Amicon® 30K Ultra-4 centrifugal filter devices (Merck, KGaA, Darmstadt, Germany) as starting sample for further protein extractions.

Protein N-glycosylation analyses by MALDI-MS

N-glycan preparation from whole serum (10 µl) or from serum purified glycoproteins (about 100 µL, as described above) consisted of glycoprotein denaturation by *Rapi*Gest™ SF Surfactant (Waters Corporation, Milford, Massachusetts) in 50 mM NH_4HCO_3 buffer, reduction in 5 mM Dithiothreitol (DTT, Sigma) at 56 °C for 30 min, alkylation in 15 mM iodoacetamide (IAA, Sigma) in the dark at room temperature for 45 min, and peptide-N-glycosydase F (PNGase F) digestion, (2-4 U, Roche, Molecular Biochemicals, Mannheim, Germany) overnight at 37°C. The released glycans were therefore purified from the resulting mixture by a 1 cc C18 Sep-Pak cartridge (Waters, Milford, MA), followed by a further purification by solid-phase-extraction (SPE) on HyperSep™ Hypercarb™ (Thermo Scientific™, Bellefonte, PA, USA) 50 mg/L cartridges (Palmigiano et al., 2018a; Messina et al., 2019). The obtained N-glycans were therefore permethylated in a DMSO/NaOH slurry followed by ICH_3 addition, according to the method originally developed by Ciucanu and Kerek (1984) to enhance glycan detection sensitivity upon MALDI-MS. Mass spectra of permethylated N-glycans, dissolved in MeOH at an estimated concentration of about 10 pmol/µL, were performed using 5-chloro-2-mercaptobenzothiazole (CMBT, 10 mg/ml in 80:20 MeOH/H_2O, v/v) as matrix (Palmigiano et al., 2018a; Messina et al., 2019). MALDI TOF and MALDI TOF/TOF analyses were conducted on a 4800 Proteomic Analyzer (AB Sciex), equipped with a Nd:YAG laser operating at a wavelength of 255 nm with <500-ps pulse and 200 Hz firing rate. Mass spectra of permethylated N-glycans were acquired in positive polarity and in reflector mode, allowing detection of monoisotopic masses with mass accuracy below 75 ppm. Data were processed using DataExplorer™ 4.9 software. Structural assignments were based on molecular weight identification, knowledge of the N-glycan biosynthetic pathway and MS/MS analyses. N-glycan species were identified by bioinformatic tools, such as GlycoMod (http://web.expasy.org/glycomod/) and glycoworkbench v2.1 (Ceroni et al., 2008) and by tools provided by the consortium for functional glycomics (http://functionalglycomics.org).

Glycosylation analysis by UHPLC-ESI MS

UHPLC-ESI MS analyses were performed starting from 7.5 µL of Tf solution (extracted from patient serum as described above) and the same aliquot of fetuin from fetal calf serum (Sigma, 2 mg/mL solution in 50 mM phosphate-buffered saline, pH 7.5). Enzymatic release and labelling of N-glycans were performed by the GlycoWorks *Rapi*Fluor-MS (RFMS) N-Glycan kit (Waters Corporation, Milford, MA, USA), modifying the suggested protocol by increasing the deglycosylation time from 5 to 60 min (Messina et al., 2020). RFMS Labelled N-glycans, tagged at the glycosylamine residue of the terminal chitobiose epitope (Zhou et al., 2017; Palmigiano et al., 2018b), were separated by an UHPLC THERMO system (Ultimate 3000 LPG3400SD) coupled to an Exactive Orbitrap HESI-II mass spectrometer (Thermo Fisher Scientific Inc., Bremen, Germany). Samples were loaded on an ACQUITY UPLC Glycan BEH Amide 130 Å, 2.1 mm× 150 mm, 1.7 µm hydrophilic interaction liquid chromatography (HILIC) column (Waters

Corporation Milford, MA, USA) and eluted with a mobile phase A consisting of 50 mM ammonium formate aqueous solution (pH 4.4) and pure acetonitrile (mobile phase B). Chromatographic runs were carried out with a mobile phase A gradient ramping from 25 to 46% over 35 min at a flow rate of 0.4 ml/min at 60 °C. MS analyses were conducted under the following conditions: heater temperature 375 °C, capillary temperature 120 °C, spray voltage 1.90 kV, capillary voltage 120 V, tube lens voltage 120 V, skimmer voltage 50 V. Spectra were acquired in positive polarity, and resolution was adjusted at 70000 FWHM @200 *m/z*. We performed three runs for each analysis, and we found not substantial differences between chromatograms and spectra recorded.

Supplemental References

Ceroni, A., Maass, K., Geyer, H., Geyer, R., Dell, A., and Haslam, S.A. (2008). GlycoWorkbench: A Tool for the Computer-Assisted Annotation of Mass Spectra of Glycans. J Proteome Res *7*, 1650-1659.

Ciucanu, I., and Kerek, F. (1984). A simple and rapid method for the permethylation of carbohydrates. Carb Res. *131*, 209-217.

Juszczak, A., Pavić, T., Vučković, F., Bennett, A.J., Shah, N., Pape Medvidov, E., Groves, C.J., Šekerija, M., Chandler, K., Burrows, C., et al. (2019). Plasma Fucosylated Glycans and C-Reactive Protein as Biomarkers of HNF1A-MODY in Young Adult-Onset Nonautoimmune Diabetes. Diabetes Care. *42*, 17-26.

Messina, A., Palmigiano, A., Bua, R.O., Romeo, D.A., Barone, R., Sturiale, L., Zappia, M., and Garozzo, D., (2019) CSF N-Glycoproteomics Using MALDI MS Techniques in Neurodegenerative Diseases. In: Santamaría E., Fernández-Irigoyen J. (eds) Cerebrospinal Fluid (CSF) Proteomics. Methods in Molecular Biology. *2044*, 255-272. Humana, New York, NY. https://doi.org/10.1007/978-1-4939-9706-0_16.

Messina, A., Palmigiano, A., Esposito, F., Fiumara, A., Bordugo, A., Barone, R., Sturiale, L., Jaeken, J., and Garozzo, D. (2020). HILIC-UPLC-MS for high throughput and isomeric N-glycan separation and characterization in Congenital Disorders Glycosylation and human diseases. Glicoconj J. https://doi.org/10.1007/s10719-020-09947-7.

Palmigiano, A., Messina, A., Bua, R.O., Barone, R., Sturiale, L., Zappia, M., and Garozzo, D. (2018a). CSF N-Glycomics Using MALDI MS Techniques in Alzheimer's Disease. In: Perneczky R. (eds) Biomarkers for Alzheimer's Disease Drug Development. Methods in Molecular Biology. *1750*, 75-91. Humana Press, New York, NY. https://doi.org/10.1007/978-1-4939-7704-8_5.

Palmigiano, A., Messina, A., Sturiale, L., and Garozzo, D. (2018b) Advanced LC-MS Methods for N-Glycan Characterization. In: Cappiello, A., Palma, P. (eds.). Comprehensive Analytical ChemistryAdvances in the Use of Liquid Chromatography Mass Spectrometry (LCMS): Instrumentation Developments and Applications. 79, pp. 147–172. Elsevier B.V., Amsterdam. https://doi.org/10.1016/bs.coac.2017.06.009.

Sturiale, L., Barone, R., Palmigiano, A., Ndosimao, C.N., Briones, P., Adamowicz, M., JaekenL, J., and Garozzo, D. (2008). Multiplexed glycoproteomic analysis of glycosylation disorders by sequential yolk immunoglobulins immunoseparation and MALDI-TOF MS. Proteomics *8*, 3822-3832.

Sturiale, L., Bianca, S., Garozzo, D., Terracciano, A., Agolini, E., Messina, A., Palmigiano, A., Esposito, F., Barone, C., Novelli, A., et al. (2019). ALG12-CDG: novel glycophenotype insights endorse the molecular defect. Glycoconj J. *36*, 461-472.

Van Eijk, HG., Van Noort, WL, Dubelaar, M-L, and Van der Heul, C. (1983). The microheterogeneity of human transferrins in biological fluids. Clin. Chim. Acta. *132*, 167-172.

Wada, Y., Azadi, P., Costello, C.E., Dell, A., Dwek, R.A., Geyer, H., Geyer, R., Kakehi, K., Karlsson, N.G., Kato, K., et al. (2007). Comparison of the methods for profiling glycoprotein glycans--HUPO Human Disease Glycomics/Proteome Initiative multi-institutional study. Glycobiology *17*, 411-422.

Zhou, S., Veillon, L., Dong, X., Huang, Y., and Mechref, Y. (2017). Direct comparison of derivatization strategies for LC-MS/MS analysis of N-glycans. Analyst. *142*, 4446–4455.